Experimental Studies of Gypsum Plasterboards and Composite Panels under Fire Conditions

Prakash Kolarkar and Mahen Mahendran
Faculty of Science and Engineering
Queensland University of Technology, Brisbane, QLD 4000, Australia

Abstract: Gypsum plasterboards are commonly used to protect the light gauge steel framed walls in buildings from fires. Single or multiple plasterboards can be used for this purpose while recent research has proposed a composite panel with a layer of external insulation between two plasterboards. However, a good understanding of the thermal behaviour of these plasterboard panels under fire conditions is not known. Therefore 15 small scale fire tests were conducted on plasterboard panels made of 13 mm and 16 mm plasterboards and four different types of insulations with varying thickness and density subject to standard fire conditions in AS 1530.4. Fire performance of single and multiple layers of gypsum plasterboards was assessed including the effects of interfaces between adjacent plasterboards. Effects of using external insulations such as glass fibre, rockwool and cellulose fibre were also determined. The thermal performance of composite panels developed from different insulating materials of varying densities and thicknesses was examined and compared. This paper presents the details of the fire tests conducted in this study, and their valuable time-temperature data for the tested plasterboard panels. These data can be used for the purpose of developing and validating accurate thermal numerical models of these panels.

Keywords: *Gypsum plasterboard, Composite panels, Insulation, Standard fire tests, Thermal performance.*

Corresponding author's email address: m.mahendran@qut.edu.au

1. Introduction

Fire resistance of non-load bearing and load bearing light gauge steel frame (LSF) wall systems depends very much on the level of protection provided to the steel frame against fire attack. The most popular method of providing this protection to the steel frame is by attaching single or multiple gypsum plasterboard sheets on either side of the frame. The walls are usually exposed to fire from one side and thus the plasterboards form the first line of defence by protecting the light gauge steel studs from high temperatures. A significant drop in temperature occurs across the thickness of each layer of plasterboard due to the dehydration of gypsum board [1]. This leads to a temperature gradient across the depth of the wall. With prolonged exposure to fire the plasterboards calcine and develop cracks allowing the heat to penetrate, eventually leading to the failure of the wall [1]. Hence the thermal performance of plasterboards plays a major role in the fire resistance of LSF wall systems. Plasterboards are also used in other forms of construction such as timber framed wall systems for the same reason. In this research many fire tests of plasterboard panels were conducted under standard fire conditions based on AS1530.4 [2] to improve the knowledge and understanding of their thermal performance. They were performed on Type X gypsum plasterboards under the product name FireStop [3]. Thermal performance of single, double and triple layers of plasterboards was investigated. Recently a composite panel was developed in which an insulation layer was used between two sheets of plasterboard [4]. These composite panels were also tested here to determine whether they provide a greater protection to LSF walls.

Gypsum plasterboards are commonly used due to their non-combustible core and fire resisting properties. The core of plasterboards is made of Gypsum, i.e. Calcium Sulphate Dihydrate ($CaSO_4.2H_2O$), a naturally occurring non-combustible mineral. The core is sandwiched between two layers of paper, which are chemically and mechanically bonded to the core to form flat sheets. The papers provide sufficient tensile strength to the board in handling and transportation. Gypsum contains approximately 21% by weight chemically bound water of crystallization and about 79% Calcium Sulphate, which is inert below a temperature of 1200^oC [5]. In addition to the water of crystallization, up to 4% free water is also present inside gypsum,

depending upon the ambient temperature and relative humidity [6-8]. The fire retarding property of the gypsum board primarily stems from this water content (free water and water of crystallization).

When the gypsum board is exposed to fire, the free water and the water of crystallization are gradually released and evaporated. The release of water known as dehydration occurs in two phases. In the first phase known as calcination, Gypsum dihydrate loses some water to yield Gypsum Hemihydrate ($CaSO_4.1/2H_2O$).

$$CaSO_4.2H_2O \longrightarrow CaSO_4.1/2H_2O + 3/2\ H_2O \quad (1)$$

The chemical reactivity of the gypsum board strongly depends on the composition of the gypsum board and the heating rate [8-10]. Thus, the first dehydration reaction can occur at temperatures above 80^oC and consumes large amounts of energy in order to evaporate the free water and the chemically bound water of crystallization. This absorption of energy delays the heat transmission through the board and causes a temperature plateau on the unexposed face of the board. The length of this plateau is a function of its thickness, density and composition, and is commonly referred to as the 'Time Delay' [11]. Calcination leads to shrinkage and loss of strength of the plasterboard [1]. The progress of calcination through the plasterboard thickness is retarded by the exterior layer of calcined Gypsum on the fire exposed side, which acts as a protective layer and adheres well with the inner uncalcined layers [1]. The second phase of dehydration, i.e. complete dehydration, occurs when the Gypsum hemihydrate is transformed to Gypsum anhydrite.

$$CaSO_4.1/2H_2O \longrightarrow CaSO_4 + 1/2H_2O \quad (2)$$

This reaction occurs at about 210^oC according to Andersson and Jansson [12] and at about 600^oC according to Sultan [13]. Wakili et al. [14] found that the second peak found by Sultan [13] is not due to the second dehydration reaction at 670^oC, but is due to the decomposition of Calcium Carbonate. There is a third peak in specific heat due to the decomposition of Calcium Carbonate as shown by the following reaction [14].

$$CaCO_3 \longrightarrow CaO + CO_2 \quad (3)$$

Decomposition of Calcium Carbonate is likely to have little effect on the thermal behaviour of gypsum plasterboard as ablation starts to occur at about 700ºC. The material may be ablated before the decomposition of Calcium Carbonate occurs. In this case, the remaining gypsum plasterboard does not benefit from the heat absorbed due to the decomposition of Calcium Carbonate (Equation 3).

There is significant discrepancy among the researchers about the second dehydration reaction and specific heat peak values of plasterboard [12-15]. Hence Keerthan and Mahendran [16] conducted specific heat tests for the Australian plasterboards, and found that the first and second dehydrations occur at 100 to 150ºC and 150 to 200ºC, respectively. They also found that at about 400ºC, a third, exothermic reaction occurs, in which the molecular structure of the soluble crystal restructures itself into a lower insoluble energy state. This observation is simliar to Manzello et al.'s [17] and Kontogeorgos and Founti's [18] findings.

There is a need to gain a full understanding of the thermal performance of panels made of multiple plasterboards and composite panels so that suitable plasterboard panels can be used with LSF walls to protect them from fires. This research forms part of a larger research project on the structural and thermal performance of LSF wall panels made of Australian high strength steels and plasterboards. Both full scale fire tests and numerical analyses were undertaken on LSF wall panels and their components. This paper presents the details of the experimental study of the thermal performance of gypsum plasterboards and composite panels under fire conditions. It also examines and compares the thermal performance of composite panels developed from different insulating materials of varying densities and thicknesses, and makes suitable recommendations.

2. Fire Tests of Plasterboards and Composite Panels

2.1. Fire Test Details

Fifteen small scale specimens of dimensions 1350 mm x 1080 mm were used in the tests as shown in Table 1. They were built using either single or multiple plasterboards or composite panels using different types of insulations placed between the plasterboards. Fire tests were conducted by exposing one face of the specimens to heat in a propane-fired vertical gas furnace. An adapter of internal dimensions 1290 mm x 1010 mm was specially designed to fit into the large furnace to isolate a single burner and facilitate the testing of small scale specimens of plasterboards and composite panels (Figure 1). The specimen was mounted on a platform extending from the base of the adapter such that it would enclose the open furnace chamber. Insulations were provided along the top and bottom edges of the specimen. The furnace temperature was measured using four Type K mineral insulated and metal sheathed thermocouples, located at the centres of the four quarters. The distance of the hot junction of the furnace thermocouples from the fire surface of the test specimen was about 100 mm. The average temperature rise of these thermocouples served as the input to the computer controlling the furnace heat according to the standard time-temperature curve given in AS 1530.4 [2], which is similar to that in ISO 834-1 [19] and ASTM E119 [20]. Four additional thermocouples were used in the chamber to give a reliable indication of the average temperature of the furnace chamber near the test specimen. These thermocouples were connected to the data logger and used in plotting the furnace time-temperature graphs. Temperatures were measured at various locations across the thickness of the specimens during the test. Figure 1 shows a typical test arrangement. Tests were stopped once the plasterboard paper on the ambient side started burning.

2.2. Details of Plasterboard Test Specimens

Test Specimens 1 and 2 were made of a single layer of 13 mm and 16 mm thick gypsum plasterboards, respectively. Test Specimen 3 consisted of 13 mm (exposed side) and 16 mm (ambient side) thick layers of gypsum plasterboards connected by 30

mm long screws spaced at 300 mm centres along the periphery. Test Specimen 4 included two 16 mm plasterboards connected together by 40 mm long screws spaced at 300 mm centres. In Test Specimen 5 three 16 mm plasterboards were firmly attached together using 50 mm long screws spaced at 300 mm centres along the edges.

K type wire thermocouples were positioned to measure the temperature profiles of the exposed surface i.e. the fire side surface (FS), the interfaces between the two plasterboards (Pb1-Pb2, Pb2-Pb3), the unexposed surface, i.e. the ambient side (Amb) and also at different depths across the thickness. Thermocouples were inserted inside the plasterboard by drilling holes to the required depth at the specimen mid-height. The hot junction of the wire thermocouple was then inserted into the hole, which was then sealed off using moist powdered gypsum plasterboard. A minimum of two thermocouples was installed at any particular depth. Five thermocouples were attached to the unexposed surface of the plasterboard at its centre and each quarter point to measure the ambient surface temperature. This led to a total of 9 thermocouples in Specimen 1 while there were 13 and 11 in Specimens 2 to 4, and 5, respectively. The thermocouple locations are shown by the coloured dots in Table 1.

2.3. Results and Discussions of Plasterboard Panels

The measured temperature data were plotted in the form of temperature versus time at various depths across the specimen thickness, and temperature versus depth at selected time intervals. In the following sections, these plots are used to analyse and critically evaluate the thermal performance of plasterboard panels including the three different phases involving water expulsion and shrinkage cracking, and many other useful observations including predictions of plasterboard fall off and insulation burn-out. Test results show that the left and right thermocouples gave very similar temperature profiles due to the use of top and bottom edge insulations and relatively large test specimens (1350x1080 mm) [4]. Hence it can be considered as one dimensional heat transfer and the measured average time-temperature profiles are presented within a number of figures in the following sections. These figures also include the AS1530.4 standard time-temperature curve targeted in the tests. The measured furnace time-temperatures curves did not exactly match this target curve

due to varying levels of furnace control in these tests. However, the temperature differences are considered to be small in general. The measured furnace time-temperature curves are not plotted in these figures to eliminate any confusion. Instead they include the measured fire side (FS) plasterboard surface time-temperature curves that are commonly used in the numerical modelling of plasterboard panels.

Test Specimen 1 (13mm plasterboard)

Smoke was observed at the edges of the specimen after three minutes due to the burning of the plasterboard paper on the exposed side. The smoke subsided after the paper was completely burnt. After six minutes steam escaped from the specimen and condensed on the top of the furnace adapter (Figure 2(a)). By the end of 12 to 13 minutes the steam subsided and the specimen burnt steadily without releasing smoke or steam. After 18 minutes the ambient side paper started to discolour and the specimen was seen to bow outward (Figure 2(b)). This was caused by the shrinkage of the exposed surface following the expulsion of water. The outside paper started burning after 33 minutes and the test was stopped.

Figure 3(a) shows the measured time-temperature profiles across the plasterboard thickness. The time-temperature profiles obtained within the thickness of the specimen at a distance of 7 mm from the fire side and on the ambient surface show the development of the temperature in three phases. The first phase displayed a steady rise in temperature from the ambient temperature to about 100°C. This was followed by the second phase where the temperature was maintained close to 100°C thus giving a plateau. In this phase the heat energy was primarily used in converting the free and chemically bound water in the plasterboard to steam. The 7 mm and 13 mm depth profiles have their second phase extending to approximately 6 and 12 minutes, respectively. The third phase started when moisture in the plasterboard was no longer available for conversion into steam. The temperature in the third phase increased gradually reaching 450°C at 7 mm depth and 275°C on the ambient surface by the end of the test, ie. when the ambient side plasterboard paper started burning.

The thermocouple at 7 mm depth from the exposed surface did not record any sudden temperature rise in the third phase until the end. This implies that the plasterboard up

to 7 mm depth, although calcinated, was still intact and prevented any sudden ingress of heat. A temperature difference of about 350°C was observed from the exposed surface to a depth of 7 mm. With a further drop of approximately 200°C from 7 mm to 13 mm depth it gave a temperature of 275°C on the ambient surface.

Figure 3(b) shows the temperature versus depth profiles at 10 minute intervals. The profile at the end of 10 minutes shows almost a straight line from the exposed surface up to the 7 mm depth and then gradually flattening out and merging to 100°C at a depth of approximately 8.5 mm. This implies that, at the end of 10 minutes of fire exposure, the specimen still had moisture from 8.5 mm to 13 mm depth. This can be verified from Figure 3(a) which shows that the 7 mm depth profile had entered the third phase at the end of 10 minutes but the 13 mm depth profile was still in the second phase. The 20 minute profile in Figure 3(b) shows the temperature at all the depths to be above 100°C implying that moisture had been completely driven out of the entire thickness.

With the expulsion of water across the thickness, the plasterboards became more calcinated with the development of several shrinkage cracks over the surface and within the thickness. At this stage, the graph of temperature versus depth in Figure 3(b) approaches linearity. The 20 and 30 minute profiles in Figure 3(b) obtained after the expulsion of water are almost parallel, suggesting that the thermal properties of the calcinated plasterboard do not change much with temperature as long as the integrity is maintained.

Test Specimen 2 (16mm plasterboard)

Test Specimen 2 was fire tested for 78 minutes. The observations about the evolution of smoke and steam were similar to Specimen 1. The ambient surface paper started to discolour uniformly by 29 minutes, and was partially burnt at the end. The plateaus for the 4, 8, 12 and 16 mm depth profiles in Figure 4(a) extended to about 3, 7, 12 and 18 minutes, respectively. This was due to the combined effects of the plasterboard dehydration and the calcinated plasterboard layer behaving as insulation to the uncalcinated plasterboard. The latter effect is due to the reduced thermal conductivity of the calcinated plasterboard, which is almost 50% lower than that of uncalcinated

plasterboard [1,14]. Figure 4(a) shows that the 12 mm depth profile has entered the third phase at the end of 15 minutes whereas the 16 mm depth profile was still in the second phase implying the presence of moisture in the last few millimetres of the plasterboard. The 75 minute profile in Figure 4(b) approached linearity, and is almost parallel to the 30 minute profile signifying very little change to the thermal properties of plasterboard over that duration.

Test Specimen 3 (13mm and 16mm Plasterboards)

Test Specimen 3 was exposed to fire for 171 minutes. The fire side paper of the exposed plasterboard caught fire by 3 minutes when the temperature of the exposed surface was about 400°C. The smoke was soon followed by steam for 4 to 5 minutes. After 20 minutes, smoke reappeared due to the burning of plasterboard paper on the ambient side of Pb1 (Plasterboard 1). The unexposed surface started to discolour when its temperature was about 200°C after 62 minutes. By the end, the ambient surface paper had blackened uniformly. Horizontal and vertical folds in the paper indicated that deep cracks in the plasterboard had reached the ambient surface with only the paper holding them together.

In Figure 5(a) the plateaus for the 7, 13, 21 and 29 mm depth profiles extended to about 6, 14, 31 and 54 minutes, respectively. Plasterboard 2 showed extended periods of plateau as explained for the last test. Since the 29 mm depth profile had a larger calcinated thickness than the 7 mm depth profile, the plateau for the former is longer than in the latter (54 versus 6 minutes).The 13 mm curve in Figure 5(a) shows the time-temperature profile of the interface (Pb1-Pb2). A temperature drop of approximately 400°C was observed from the exposed surface to the ambient side of Plasterboard 1 (i.e. Pb1-Pb2 interface) and a further drop of about 550°C to the unexposed surface by the end of the test. Both plasterboards remained intact.

The 7 mm and 13 mm depth temperature profiles of Specimen 3 display higher temperatures than the equivalent depth temperature profiles of Specimen 1 at corresponding times. This is due to the influence of Plasterboard 2 in Specimen 3, which blocks the heat and redirects most of it to Plasterboard 1 causing it to heat up

faster. The observations based on Figure 5(b) are similar to those made for Specimens 1 and 2.

Test Specimen 4 (Two 16mm Plasterboards)

Test Specimen 4 was subjected to fire for 222 minutes. Its behaviour was similar to Specimen 3. After intermittent evolution of smoke and steam, the ambient side started to discolour after 78 minutes. Figure 6(a) shows the time-temperature profiles across the specimen cross-section while Figure 6(b) shows the temperature-depth profiles at specific time intervals. The plateaus for 8, 16, 24 and 32 mm depth profiles were seen to extend to 6, 23, 40 and 60 minutes, respectively. Plasterboard 2 showed considerably extended periods of plateau. The length of plateau increased with plasterboard depth due to the same reasons given in the last test. At the end a temperature difference of about 320°C was noticed across Plasterboard 1 and 630°C across Plasterboard 2. Both plasterboards were intact until the end. As expected the 8 mm and 16 mm depth temperature profiles showed higher temperatures than the equivalent depth profiles of Specimen 2 at corresponding times due to the heat redirected by the ambient side plasterboard.

Test Specimen 5 (Three 16mm Plasterboards)

Test Specimen 5 was subjected to fire testing for about 3 hours. Figure 7(a) shows the time-temperature profiles across the thickness at various depths. The 16, 32 and 48 mm depth temperature profiles show their second phases extending up to 23, 62 and 120 minutes, respectively. Plasterboard 1 heated up quite rapidly with its temperature reaching 900°C by 155 minutes. After 165 minutes Plasterboard 1 must have partially or fully collapsed as the curve rose rapidly and merged with the fire side (FS) curve. At the end, the temperature at the Pb2-Pb3 interface had reached 750°C while the unexposed surface reached 200°C. In Figure 7(b) the temperature-depth curves are more linear up to 120 minutes. Beyond 150 minutes Plasterboard 1 deteriorated very rapidly forcing the portion of graph between 0 to 16 mm (representing Pb1) to become horizontal. At 180 minutes the initial portion from 0 to 16 mm was horizontal, signifying that Pb1 had collapsed and was no longer effective. The temperature drop from 16 mm to 32 mm and from 32 mm to 48 mm signifies the presence of Plasterboards 2 and 3 until the end. The advantage of three plasterboard

layers over two layers is observed only during the initial two hours due to the extended plateau of the temperature profile on the ambient surface. After two hours this advantage was reduced rapidly, and by three hours both specimens are equivalent and displayed similar thermal performance.

2.4. Details of Composite Panel Test Specimens

Test Specimen 6 is a composite panel formed by sandwiching a layer of insulation between two 16 mm plasterboards. This was achieved by first fixing 16 mm plasterboard strips of 50 mm width along the periphery of the exposed plasterboard (Pb1) to form a cavity (Figure 8). The desired cavity depth was obtained by using the appropriate thickness and number of plasterboard strips along the border. In this test specimen a 32 mm cavity was provided using two 16 mm strips. The strips were then fixed to Pb1 using 50 mm long screws at 300 mm centres. Glass fibre insulation in the form of a 50 mm thick mat of 13.88 kg/m^3 density was then laid inside the cavity (Figure 8), and compressed to a thickness of 32 mm by firmly pressing it with the second 16 mm plasterboard (Pb2). This plasterboard was then screwed to the frame by 70 mm long screws at 300 mm centres. Compressing the 50 mm thick glass fibre mat to 32 mm thickness increased its density from 13.88 to 21.68 kg/m^3. Thermocouple wires were carefully installed in the interfaces between plasterboard and insulation to obtain the temperature profiles on either side of the insulation.

Test Specimen 7 was built in a manner similar to Test Specimen 6. However, two 50 mm glass fibre mats were laid in a cavity of depth 32 mm. They were compressed to a thickness of 32 mm by the use of washers held down by screws passing through the base plasterboard. The compressed glass fibre mat was further compressed by fixing the second plasterboard. Compressing the glass fibre mats from a combined thickness of 100 mm to 32 mm increased its density from 13.88 to 43.4 kg/m^3. This test specimen was built to study the effect of insulation density on the fire performance.

Specimens 8 and 9 were built in a similar manner to Specimens 6 and 7. In Specimen 8, 25 mm thick semi-rigid glass fibre mat of density 37 kg/m^3 was used as insulation while 13 mm glass fibre board of density 168 kg/m^3 was used in Specimen 9.

Test Specimen 10 was built using 25 mm thick rockwool insulation of density 100 kg/m^3 while Test Specimen 11 was built using 13 mm thick rockwool insulation of density 114 kg/m^3. Test Specimens 12 to 14 were built using cellulose fibre insulation with a thickness of 32 mm (density = 102 kg/m^3), 25 mm (density = 108 kg/m^3) and 20 mm (density = 131 kg/m^3), respectively. The insulation was wet sprayed onto the plasterboards using a special wall nozzle. Insulation thickness and density were varied to study their effect on the fire performance. Test Specimen 15 was built using 25 mm thick Isowool insulation. The purpose of using this high quality insulation was to compare the performance of insulations. Eleven thermocouples were used to study the temperature gradient across each composite panel (Specimens 6 to 15).

2.5. Results and Discussions of Composite Panels

Test Specimens 6 to 9 (Composite Panels with Glass Fibre Insulation)

Test Specimens 6 to 9 were exposed to the standard fire for about three hours. Their initial behaviour was similar to the previously tested specimens. All the specimens displayed a small amount of thermal bowing near the end of the test. The ambient surface showed uniform discolouration after about 110 minutes (Figure 9(a)). The glass fibre insulation in all the specimens was almost completely consumed by heat with only small amounts still visible along the edges of the specimens (Figure 9(b)). Figures 10 (a) to (d) show the time-temperature graphs of Specimens 6 to 9.

The time-temperature graphs show that the interface between Plasterboard and Insulation (Pb1-Ins) in all the specimens showed a very rapid rise in temperature in the third phase crossing 600°C at about 35 minutes. The temperature profile of Pb1-Ins tended to become horizontal when its temperature approached 700°C. The glass fibre insulation at this temperature began to disintegrate and lose its insulating properties as seen from the temperature-depth profiles in Figure 11. The central parts of the graphs representing the insulation tended to become horizontal from 90 minutes onwards for Specimens 6 to 8 and 109 minutes for Specimen 9 indicating that the insulation was no longer capable of causing a temperature drop across its thickness.

As the heat energy was used in disintegrating the glass fibre insulation, the temperature on the ambient side of Pb1 (i.e. Pb1-Ins) did not rise. Also less heat was getting redirected due to the continuous loss of insulation. These factors kept the temperature on the ambient side of Pb1 steady (under 700°C) almost until the end of the test. The temperatures of the two interfaces, Pb1-Ins and Ins-Pb2, merged together soon after the disintegration of the glass fibre insulation due to direct transmission of heat by radiation. Regardless of insulation thickness and density, the glass fibre insulation became ineffective at about 700°C making the composite panels follow similar time-temperature profiles until the end of the test. In all the specimens Pb1 and Pb2 remained intact until the end.

The temperature development on the ambient side of the insulation (Ins-Pb2) in Test Specimens 6 to 9 is shown in Table 2 at 10 minute intervals. Table 2 shows that the thickness, the number of layers or the density of glass fibre insulation does not significantly affect the temperature development of the Ins-Pb2 interface. In the initial stages the insulation in Test Specimen 9 performed slightly better than those in other tests. However, this advantage was lost when the fire side temperature of the insulation reached 700°C. The temperatures on the ambient side of the insulation in all the test specimens were similar after the fire side of the insulation reached 700°C. Hence the thermal performance of the glass fibre insulated composite panels can be assumed to remain unchanged regardless of the thickness or density of the insulations used. However, the use of semi-rigid glass fibre mats is recommended as the construction using them is much easier due to the ease of handling.

Test Specimens 10 and 11 (Composite Panels with Rockwool Insulation)

Test Specimens 10 and 11 were subjected to the fire for nearly three hours. Figures 12(a) and (b) show the time-temperature profiles. In Test Specimen 10 (Figure 12(a)), the Pb1-Ins profile rose rapidly in the third phase crossing 600°C by 32 minutes, beyond which it flattened out, with the temperature gradually increasing to 900°C by 147 minutes. At this time Plasterboard 1 must have collapsed as the curve rose rapidly to merge with the fire side (FS) curve. The Ins-Pb2 curve rose gradually to 600°C by 147 minutes after which the temperature rose sharply due to the collapse of Plasterboard 1. The profile of the interface Ins-Pb2 continued to maintain a

temperature difference of over 250°C with the FS curve even beyond 147 minutes, implying that the insulation was still intact and functional. The 150 mm depth temperature profile in Figure 13 shows a horizontal segment from exposed surface to 16 mm depth signifying the collapse of Plasterboard 1. Beyond 16 mm and up to 41 mm depth the temperature drop is brought about by the 25 mm insulation, and beyond 41 mm the temperature drop is due to Plasterboard 2. The thermal performance of Test Specimen 11 was very similar to Test Specimen 10 including the collapse of Pb1 (see Figures 12 and 13).

Contrary to glass fibre insulation, the rockwool insulation showed greater resistance to disintegration (Figure 14). Its physical presence was blocking and redirecting the heat flow to Plasterboard 1. This resulted in the rise of the temperature of Pb1-Ins to values beyond 700°C and steadily kept rising up to 900°C when Pb1 started to breach. Even after being directly exposed to fire following the collapse of Pb1, the insulation remained intact and continued to offer protection to Pb2. Table 3 shows the temperature profile of the ambient side of the insulation in Test Specimens 10 and 11. The thermal performance of both insulations is nearly the same despite the different thicknesses. It was different only after 145 minutes following the collapse of Pb1 in Test Specimen 10.

Test Specimens 12 to 14 (Composite Panels with Cellulose Fibre Insulation)

Tests for the cellulose fibre composite panels lasted slightly over two hours. The ambient side paper started to discolour after 100 minutes. The discolouration in all three specimens was observed to be non-uniform (Figure 15(a)) indicating the burning of cellulose fibre within the specimen in certain areas creating pockets of high temperature. This allowed the heat to penetrate the insulation compromising the integrity of the composite panel. The test was stopped soon after the burning of the ambient side paper (Figure 15(b)). In all the test specimens Pb1 had collapsed fully or partially and the cellulose fibre had completely burnt out at the end of the test leaving behind traces of ash sticking to the fire side of Pb2 (Figure 15(c)).

Figures 16(a) to (c) show the time-temperature profiles across Test Specimens 12 to 14. The profiles of Test Specimens 12 and 13 were almost identical with the plateaus

of the Pb1-Ins interface extending up to 18 minutes and crossing 600°C at about 35 minutes. By 120 minutes the ambient side temperature of Plasterboard 1 (Pb1-Ins) in Test Specimens 12 and 13 had reached about 900°C. The third phase of the Ins-Pb2 profile in Test Specimens 12 and 13 started at about 36 minutes and by 120 minutes a temperature difference of about 200°C was recorded across the insulation thickness (i.e. the difference in the temperatures of Pb1-Ins and Ins-Pb2) indicating the presence of insulation. The sudden increase in the temperature of the Pb1-Ins interface at 125 minutes for Test Specimen 12 and at 119 minutes for Test Specimen 13 indicates the breaching of the exposed plasterboard. This was soon followed by the burning of the paper on the ambient side and the test was terminated. The temperature profiles of the ambient side in Specimens 12 and 13 show the plateau extending to 90 minutes. Beyond 90 minutes, however, it rose quickly crossing 200°C by 120 minutes and 112 minutes for Specimens 12 and 13, respectively. This rapid temperature rise was probably due to the insulation burn out in certain areas creating pockets of high temperature and allowing the heat to penetrate the composite panel.

Figures 17 (a) and (b) show the temperature-depth graphs for Test Specimens 12 and 13, respectively. They are almost linear at 90 minutes. Beyond this time deterioration in the insulation can be noted in Test Specimen 12 as the profile tends to become horizontal in the central portion, although a drop of 200°C across the insulation thickness is still noted at 120 minutes. However in Test Specimen 13, beyond 90 minutes, the deterioration of Pb1 seems to have started along with the disintegration of the insulation as the initial portion of the profile from 0 to 16 mm (representing Pb1) at 120 minutes has become almost horizontal suggesting the cracking of the exposed plasterboard, whereas a temperature drop of about 300°C is seen from 16 mm to 41 mm in the profile (representing the 25 mm thick insulation), signifying the presence of the insulation.

Figure 16(c) shows that Test Specimen 14 deteriorated more rapidly when compared to Test Specimens 12 and 13. The plateau for the Pb1-Ins interface extended to 21 minutes beyond which the temperature increased rapidly crossing 600°C by 40 minutes. Beyond 600°C the temperature rise was gradual reaching 800°C by 100 minutes when the plasterboard appeared to have partially collapsed as the temperature

of the interface (Pb1-Ins) increased sharply merging with the fire side curve at 120 minutes.

The temperature profile on the ambient side had its plateau extending up to 80 minutes beyond which it started to increase quickly crossing 200°C by about 112 minutes. In Test Specimens 12 and 13 the 120 minute profile showed a fall in temperature across the entire thickness of the composite panel signifying that both the plasterboards and the insulation were still intact, whereas in Test Specimen 14 the 120 minute profile was horizontal from 0 to 36 mm indicating the collapse of Pb1 and the complete disintegration of the cellulose fibre. The temperature development on the ambient side of the insulation in Test Specimens 12 to 14 is shown in Table 4. The thermal performance of these specimens varied with changing thickness and density of insulation, unlike those built using glass fibre and rockwool. The influence of density is more dominant than the influence of thickness in the case of cellulose fibres. As there is less control in maintaining the density of the insulation layer over the entire interface it is likely that certain areas burn faster than others leading to the formation of hot pockets and thus an early insulation failure.

Test Specimen 15 (Composite Panels with Isowool Insulation)

Test Specimen 15 was subjected to the fire for about three hours. The ambient side discoloured uniformly from about 140 minutes. Figure 18(a) shows the temperature profiles at various depths. The interface temperature (Pb1-Ins) had its plateau extending to 21 minutes beyond which it increased sharply crossing 600°C at 35 minutes and reaching 700°C at 45 minutes. Beyond this point the temperature was almost constant up to 80 minutes and then increased very gradually reaching 900°C at 160 minutes. The exposed plasterboard (Pb1) must have breached at this time as the temperature of the interface (Pb1-Ins) increased suddenly merging with the fire side curve. The temperature drop across the insulation thickness at this time was about 400°C indicating that the insulation had maintained its integrity until the end. The ambient side temperature was seen to have its plateau extending to 120 minutes beyond which it increased gradually crossing 200°C at about 170 minutes.

Figure 18(b) shows the temperature-depth profile at 30 minute intervals. The 150 minute profile is linear whereas the initial portion of the 180 minute profile (from 0 to 16 mm) is horizontal, indicating the collapse of Pb1. The temperature of the interface (Ins-Pb2) and the ambient side temperature rose rapidly soon after the collapse of the external plasterboard. A comparison of the interface temperature (Ins-Pb2) of Specimen 15 with that of other specimens using glass fibre, rockwool and cellulose fibre insulation showed that Isowool insulation performed better in the initial stages because of its ability to withstand very high temperatures. However, the rising temperature of the interface (Pb1-Ins) on account of the redirected heat forced the exposed plasterboard to heat up rapidly leading to its collapse. The advantage gained by the use of superior insulation was lost soon after the collapse of the exposed plasterboard.

2.6. Summary of Results and Discussions

Previous sections have presented valuable test results in the form of time-temperature graphs at varying depths across the thickness and temperature-depth graphs at varying time intervals for plasterboard panels consisting of single and multiple plasterboards and four insulations with varying thickness and density. These graphs were used to describe the thermal performance of each panel in detail and to explain the physical behaviour involving thermal bowing, shrinkage cracking, plasterboard fall-off and insulation burn-out. These valuable time-temperature data can also be used to validate numerical models of such plasterboard panels. Following are some of the main findings.

Despite the numerous shrinkage cracks that develop over the surface and within the plasterboard thickness due to the expulsion of free and chemically bound water, the thermal gradient across the thickness is unaffected by the period of fire exposure and rising plasterboard temperature up to about 900^{o}C. Beyond this point, the plasterboard loses its integrity since the cracks are likely to get interconnected and reach the ambient surface allowing the passage of heat.

The presence of interfaces in the multiple board panels improve the fire performance by extending the duration of the temperature plateau (second phase) on the ambient

side. The interfaces, however, do not influence the linear variation of temperature across the specimen thickness after the expulsion of water as transmission of heat across the joint is very rapid on account of radiation.

The use of three plasterboards is better than two for about two hours, beyond which the external plasterboard of the triple layered specimen fell off probably due to the bending of heat softened screws under plasterboard weight. Improved fixing methods are needed if multiple layers (more than two) of plasterboards are used.

Composite panels performed better than double plasterboards as seen in Figure 19 where the temperatures on the ambient surface and the interface Ins-Pb2 or Pb1-Pb2 are shown. The plateau (second phase) of Pb2 extended to about 80 minutes for composite panels with glass fibre, rockwool and cellulose insulations compared to about 60 minutes in the case of double plasterboards with no insulation. The comparison of the times to reach the insulation failure temperature of 170ºC on the ambient surface is as follows: 100, 95 and 110 minutes versus 75 minutes. The Ins-Pb2 temperature was less than 900ºC for an extended period for composite panels, implying that the second plasterboard will protect the steel wall studs without premature fall off. This confirms the superior thermal performance of composite panels compared with double plasterboards with no insulation. Figure 19 also demonstrates the thermal improvements as the number of plasterboards is increased to three.

Glass fibre insulation disintegrated at about 700^{o}C. This resulted in similar time-temperature profiles for all the composite panels using glass fibre insulation of varying thickness and density. Both plasterboards were intact until the end of the test because the temperature of the Pb1-Ins interface did not increase beyond 750^{0}C even after the disintegration of glass fibre insulation. When rockwool and cellulose insulations were used, the external plasterboard (Pb1) fell off due to the continuous build up of the Pb1-Ins interface temperature reaching 900^{0}C caused by redirected heat from the longer lasting insulation. Following this the ambient side of the specimen increased rapidly.

Composite panels made of rock fibre insulation of varying density and thickness also did not display any appreciable difference in their thermal performances although the

insulation lasted until the end of the test. Rockwool insulation showed much greater resistance to disintegration when compared with glass fibre and cellulose fibre insulations.

Fire resistance of cellulose insulation appears to depend on its density with lower density cellulose fibres surviving longer periods. The distribution of cellulose fibres within a specimen could also be non-uniform as the spraying technique of wet cellulose fibre onto the plasterboard is not a standardized process and can lead to areas of varying density within a specimen. This was probably the cause of the burning of cellulose fibre within the specimens at different rates giving rise to pockets of high temperature and thus lowering the integrity.

3. Conclusions

This paper has presented the details of 15 fire tests on the thermal performance of plasterboards and the new composite panels subject to standard fire conditions, and the results. It included valuable time-temperature data for plasterboard panels made of single and multiple plasterboards with and without insulation. Two different plasterboard thicknesses and four types of insulations with varying thickness and density were considered in this study. Test results provided a good understanding of the thermal performance of these panels as a function of its composition and led to suitable recommendations for their use with LSF wall systems. They showed the superior performance of composite panels based on using a layer of insulation between two plasterboards. The vast amount of time-temperature data from this research can be used in the development and validation of accurate numerical models of these panels used in not only LSF wall systems but also other wall systems.

Acknowledgements

The authors would like to thank Australian Research Council for their financial support and the Queensland University of Technology for providing the necessary facilities and support to conduct this research project. They gratefully acknowledge the valuable contribution of Dr P. Keerthan in the preparation of this paper.

References

1. Kontogeorgos D., Mandilaras I., and Founti M. (2011), Scrutinizing Gypsum Board Thermal Performance at Dehydration Temperatures, Journal of Fire Sciences Vol. 29, Issue 2, pp. 111-130.
2. Standards Australia (SA) (2005), AS 1530.4, Methods for Fire Tests on Building Materials, Components and Structures, Part 4: Fire-Resistance Tests of Elements of Building Construction, Sydney, Australia.
3. Boral Pty. Ltd. (2009), Plasterboard Product Manual, Sydney, Australia.
4. Kolarkar, P. (2010), Structural and Thermal Performance of Cold-formed Steel Stud Wall Systems under Fire Conditions, PhD Thesis, Queensland University of Technology, Brisbane, Australia.
5. Gonclaves, T. Clancy, P. and Poynter, W. (1996), Mechanical Properties of Fire Rated Gypsum Board, Victoria University of Technology, Australia.
6. Buchanan, A. H. (2001), Structural Design for Fire Safety, John Wiley and Sons, Hong Kong.
7. Thomas, G.C. (2002), Thermal Properties of Gypsum Plasterboard at High Temperatures, Fire and Materials, Vol. 26, pp 37–45.
8. Mehaffy, J.R., Cuerrier, P. and Carisse, G. (1994), A Model for Predicting Heat Transfer through Gypsum-Board/Wood-Stud Walls Exposed to Fire, Fire and Materials, Vol. 18, pp. 297-305.
9. Paulik F., Paulik J., Arnold M. (1992), Thermal Decomposition of Gypsum, Thermochimica Acta Vol. 2, pp. 195–204.
10. Elbeyli I.Y., Piskin S. (2004), Thermal Dehydration Kinetics of Gypsum and Borogypsum under Non-isothermal Conditions, Chinese Journal of Chemical Engineering Vol. 12, Issue 2, pp. 302–305.
11. Gerlich, J.T. (1995), Design of Load Bearing Light Steel Frame Walls for Fire Resistance, Fire Engineering Research Report 95/3, University of Canterbury, Christchurch, New Zealand.

12. Andersson, L. and Jansson B. (1987), Analytical Fire Design with Gypsum—A Theoretical and Experimental Study, Institute of Fire Safety Design, Lund, Sweden.
13. Sultan, M.A. (1996), A Model for Predicting Heat through Non-insulated Unloaded Steel-Stud Gypsum Board Wall Assemblies Exposed to Fire, Fire Technology, Vol. 32, No. 3, pp. 239-259.
14. Wakili, K.G., Hugi, E., Wullschleger, L. and Frank, T.H. (2007), Gypsum Board in Fire—Modelling and Experimental Validation, Journal of Fire Sciences, Vol. 25, pp. 267–282.
15. Cooper, L.Y. (1997), The Thermal Response of Gypsum-Panel/Steel Stud Wall Systems Exposed to Fire Environments – A Simulation for the use in Zone-Type Fire Models, NIST Report NISTIR 6027, Building and Fire Research Laboratory, National Institute of standards and Technology, Gaithersburg, USA.
16. Keerthan, P. and Mahendran, M. (2010), Numerical Studies of Gypsum Plasterboards under Fire Conditions, Research Report, Queensland University of Technology, Brisbane, Australia.
17. Manzello, S.L., Richard, G.G., Scott, R.K. and David B.L. (2008), Influence of Gypsum Board Type (X or C) on Real Fire Performance of Partition Assemblies, Fire and Materials, Vol. 31, pp. 425-442.
18. Kontogeorgos D.A. and Founti M.A. (2012), Gypsum Board Reaction Kinetics at Elevated Temperatures, Thermochimica Acta, 529, pp. 6-13
19. ISO 834 (1999), Fire Resistance Tests – Elements of Building Construction, International Organisation for Standardisation, Switzerland.
20. ASTM E119 (1995), Standard Test Methods for Fire Tests of Building Construction and Materials, West Conshohocken, PA, USA.

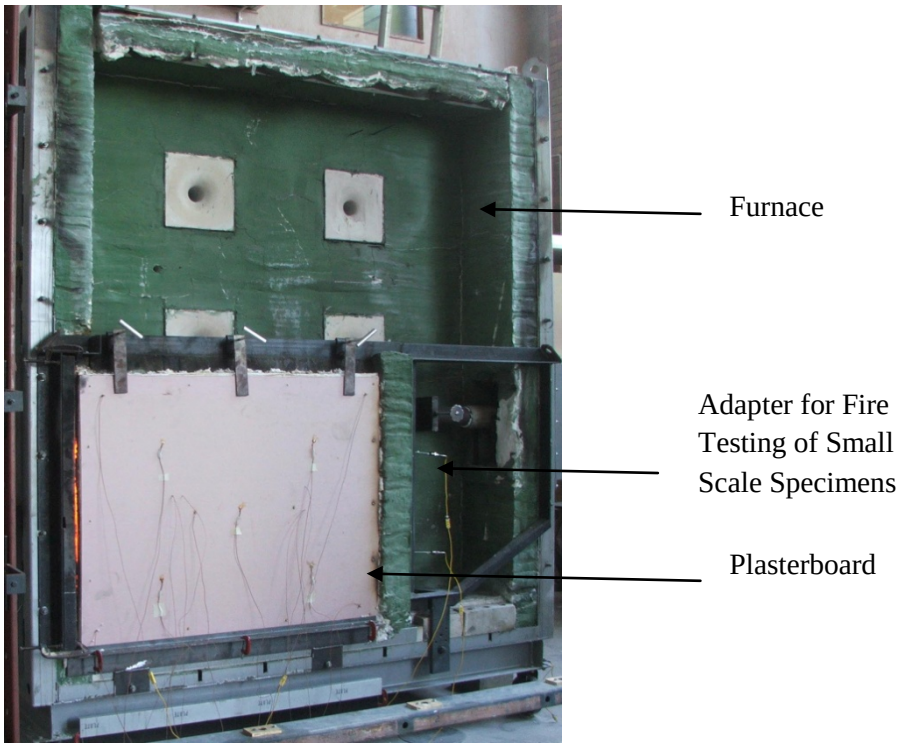

Figure 1: Fire Test Set-up of Plasterboards and Composite Panels

(a) Test after 3 Minutes.

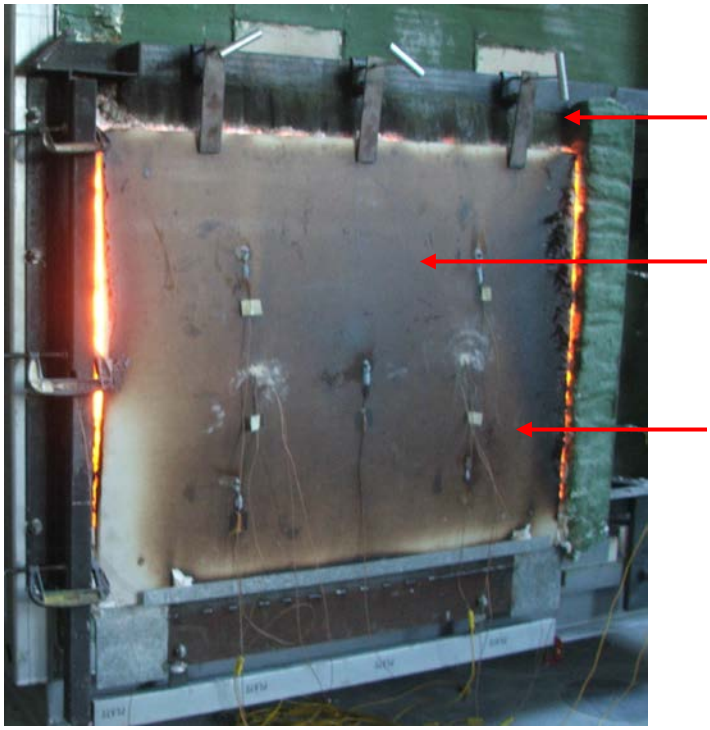

(b) Thermal Bowing at the End of Test

Figure 2: Fire Testing of Test Specimens 1 to 4

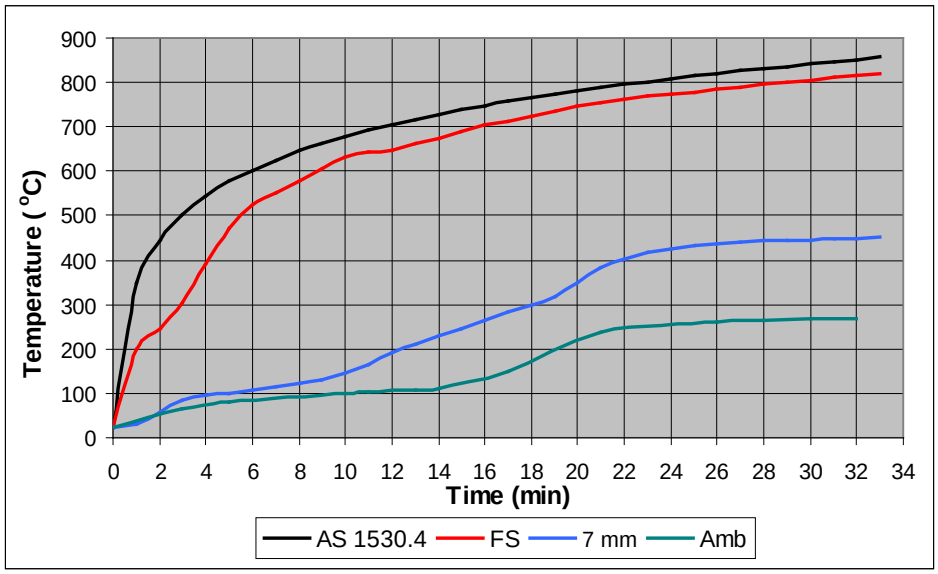

(a) Time - Temperature Profiles

Note: AS 1530.4: Standard time-temperature curve from AS 1530 Part 4

FS : Temperature profile of the exposed surface of the specimen (Fire Side surface)

7 mm: Temperature profile at a depth of 7 mm from the exposed surface

Amb: Temperature profile of the unexposed surface of the specimen

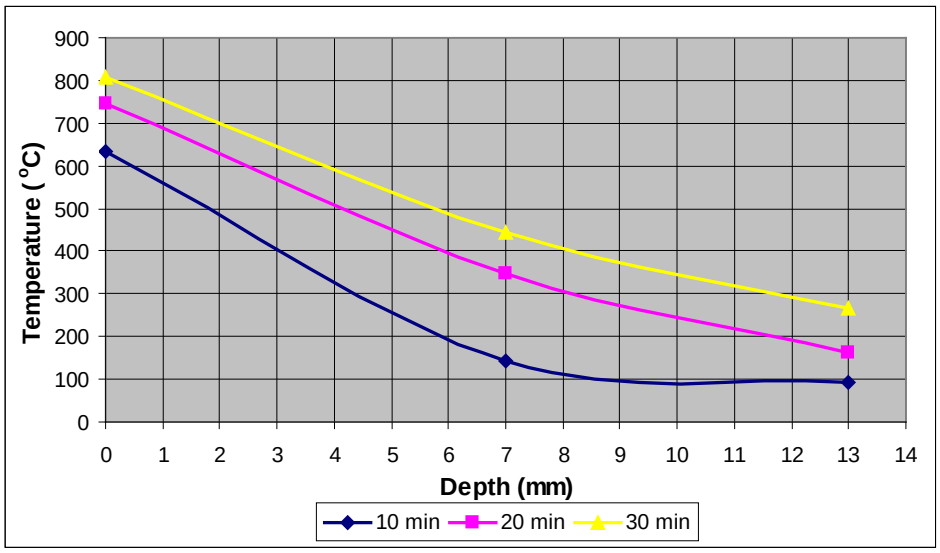

(b) Temperature - Depth Profiles

Figure 3: Temperature Profiles of Test Specimen 1

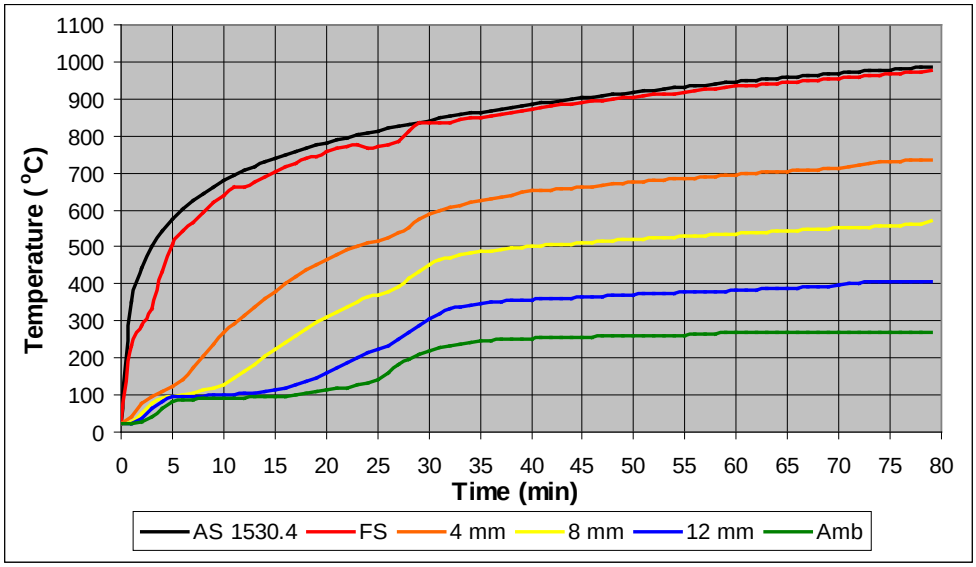

(a) Time - Temperature Profiles

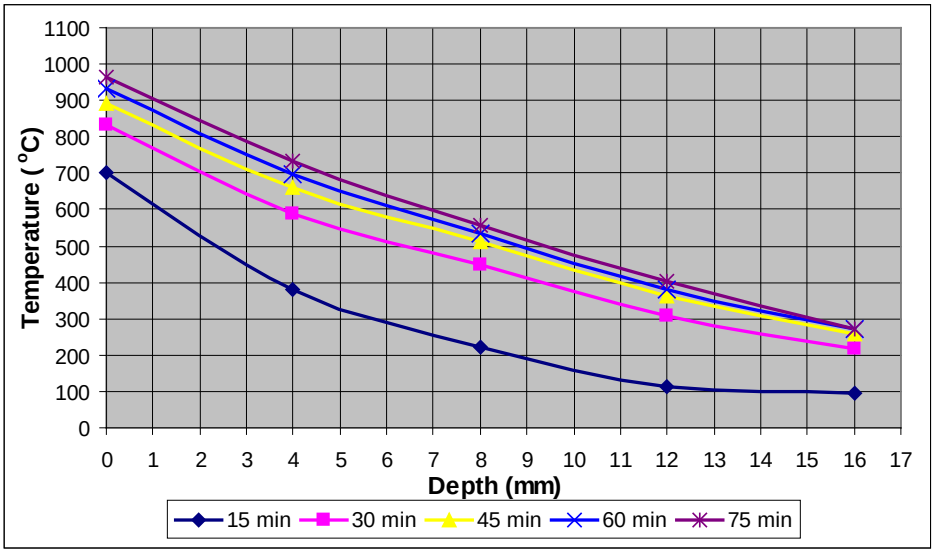

(b) Temperature - Depth Profiles

Figure 4: Temperature Profiles of Test Specimen 2

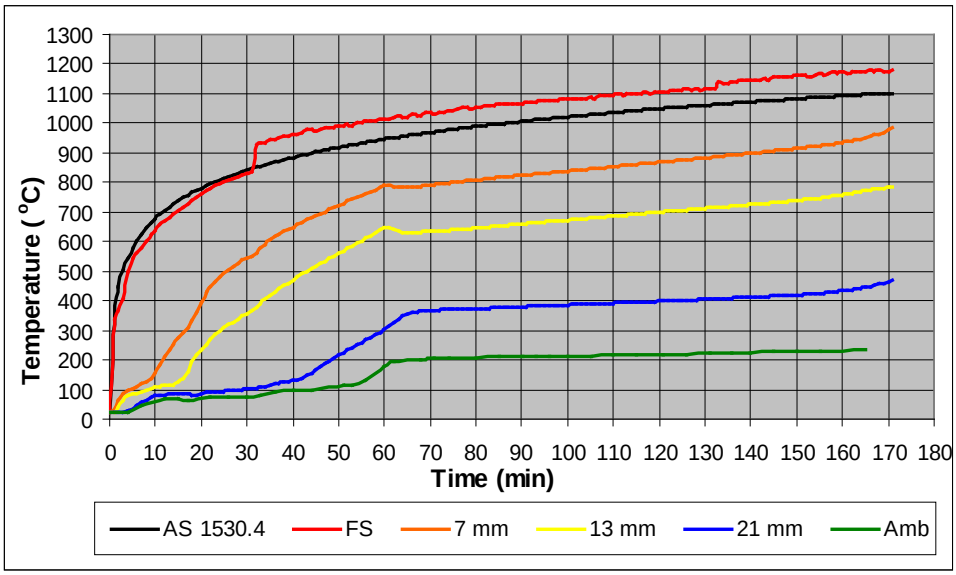

(a) Time - Temperature Profiles

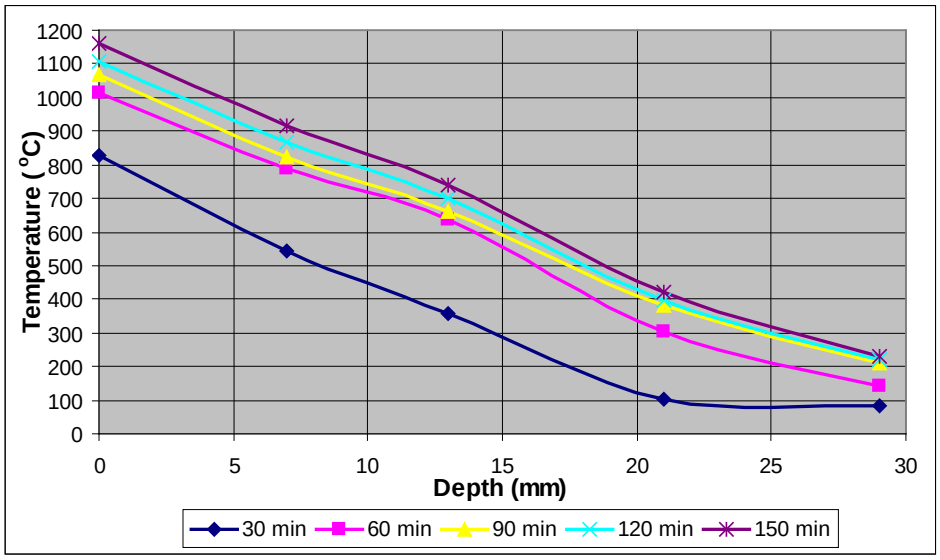

(b) Temperature - Depth Profiles

Figure 5: Temperature Profiles of Test Specimen 3

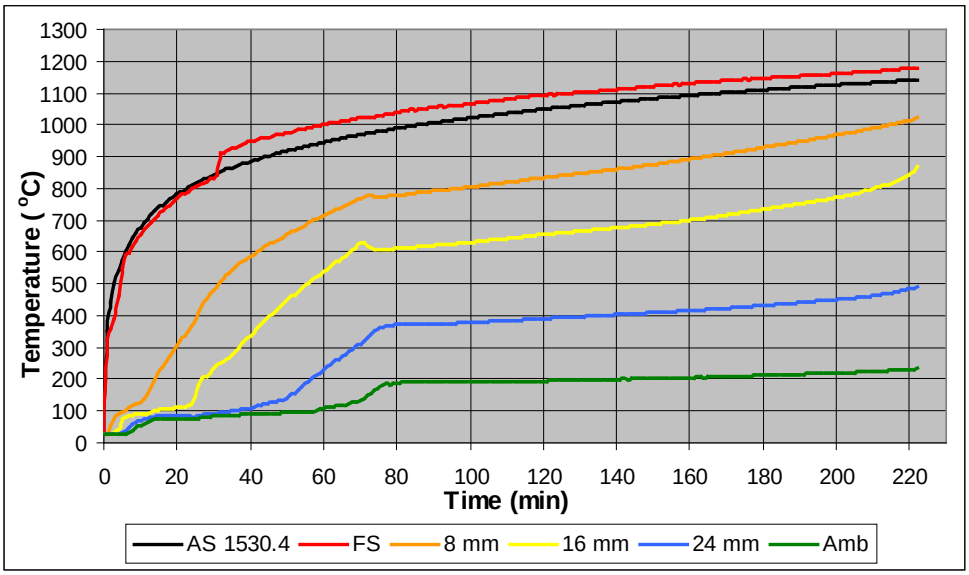

(a) Time - Temperature Profiles

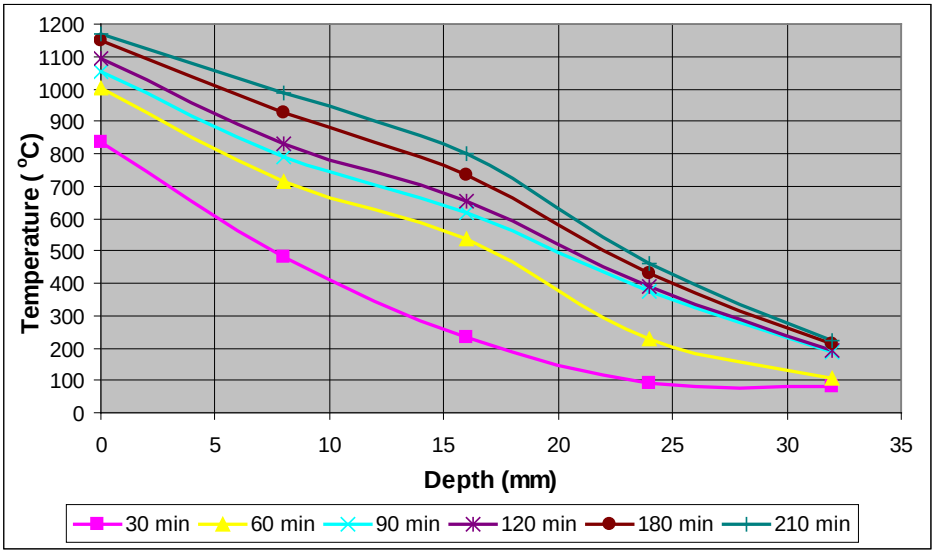

(b) Temperature - Depth Profiles

Figure 6: Temperature Profiles of Test Specimen 4

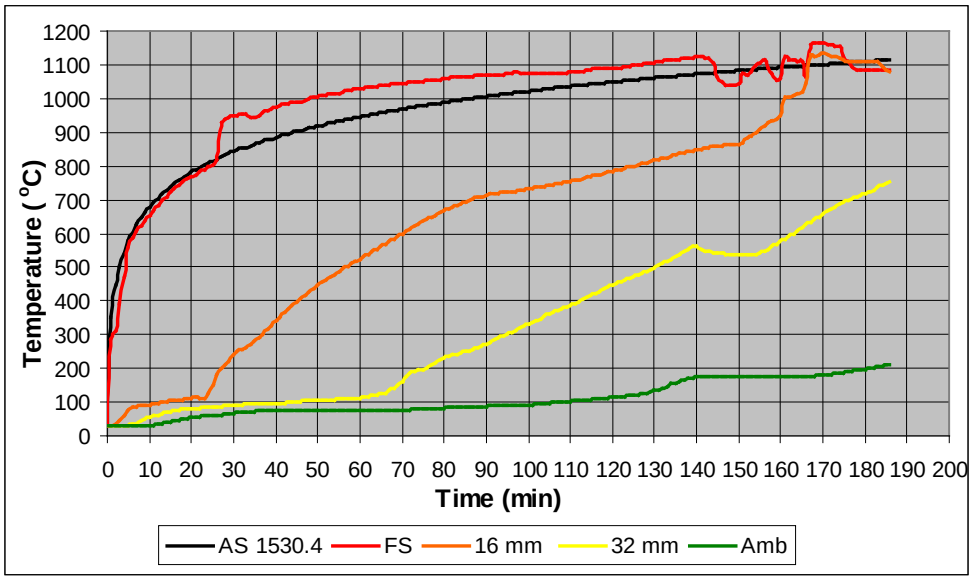

(a) Time - Temperature Profiles

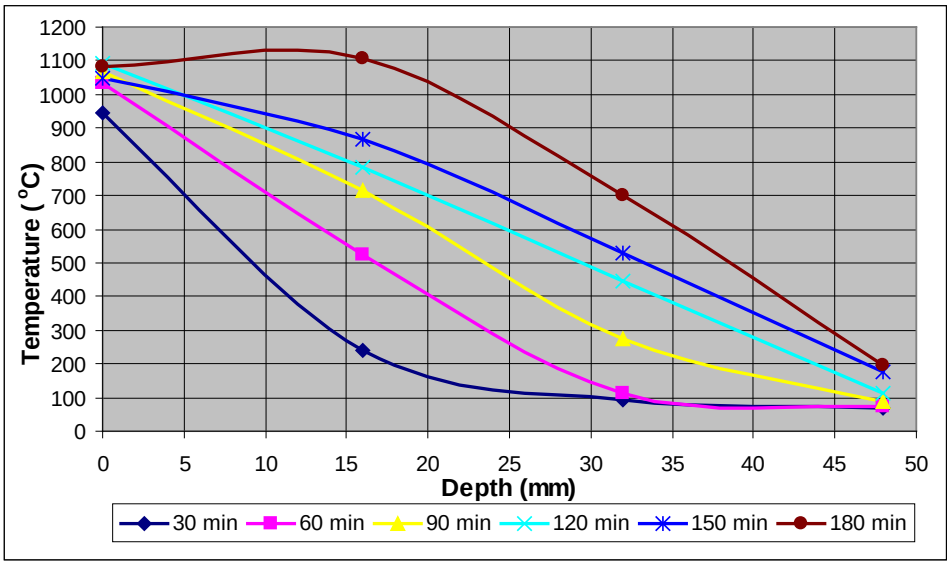

(b) Temperature - Depth Profiles

Figure 7: Temperature Profiles of Test Specimen 5

Figure 8: Construction of Test Specimen 6

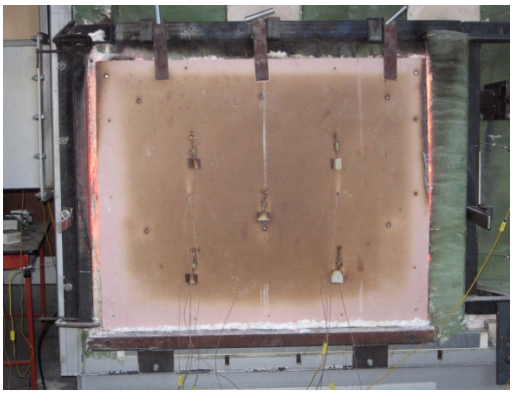

(a) Uniform Discolouration of Paper on Ambient Side

(b) Glass Fibre Insulation is totally burnt Leaving a Dark Stain Behind

Figure 9: Fire Testing of Test Specimens 6 to 9

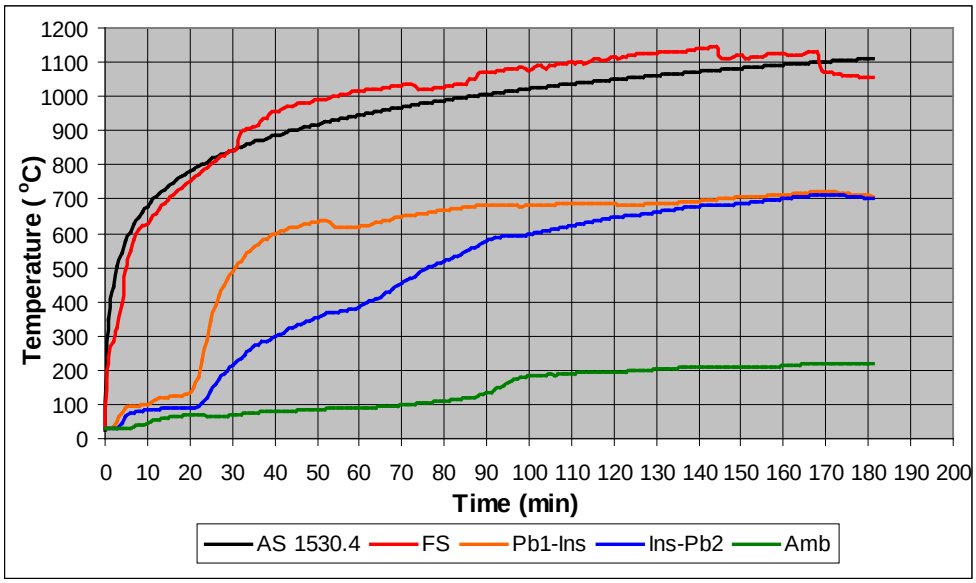

(a) Test Specimen 6

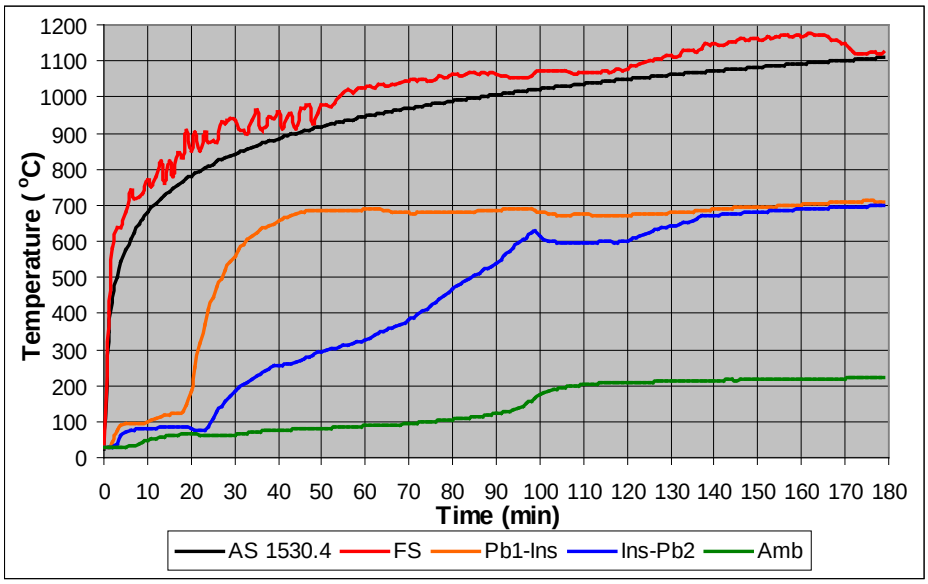

(b) Test Specimen 7

Note: Pb1-Ins: Temperature profile of the interface between Pb1 and the insulation
Ins-Pb2: Temperature profile of the interface between the insulation and Pb2

Figure 10: Time - Temperature Profiles of Test Specimens 6 to 9

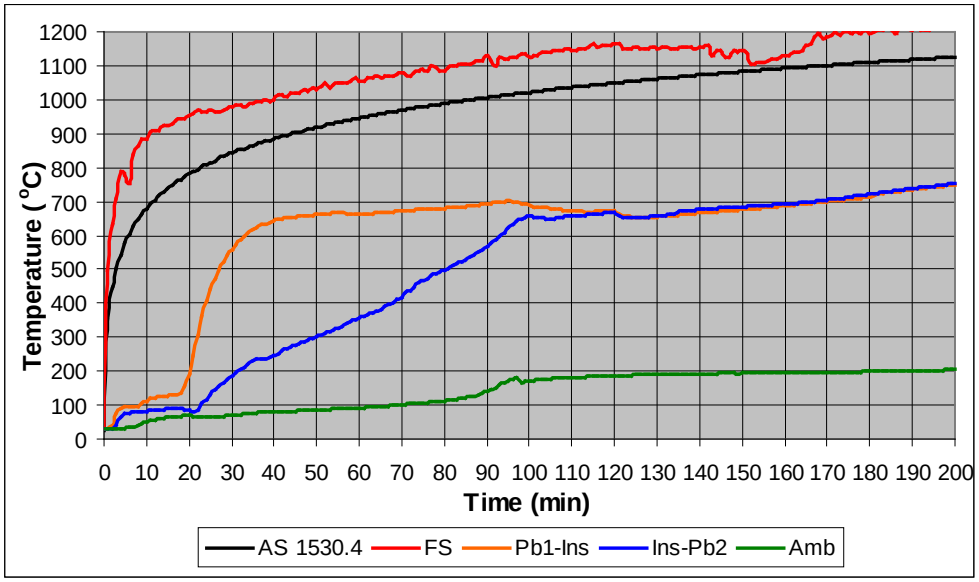

(c) Test Specimen 8

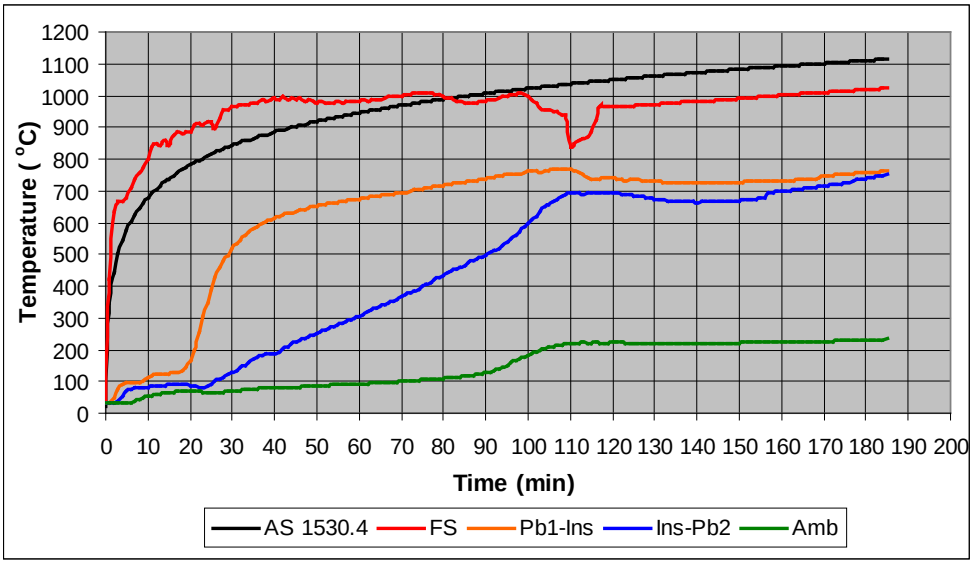

(d) Test Specimen 9

Figure 10: Time - Temperature Profiles of Test Specimens 6 to 9

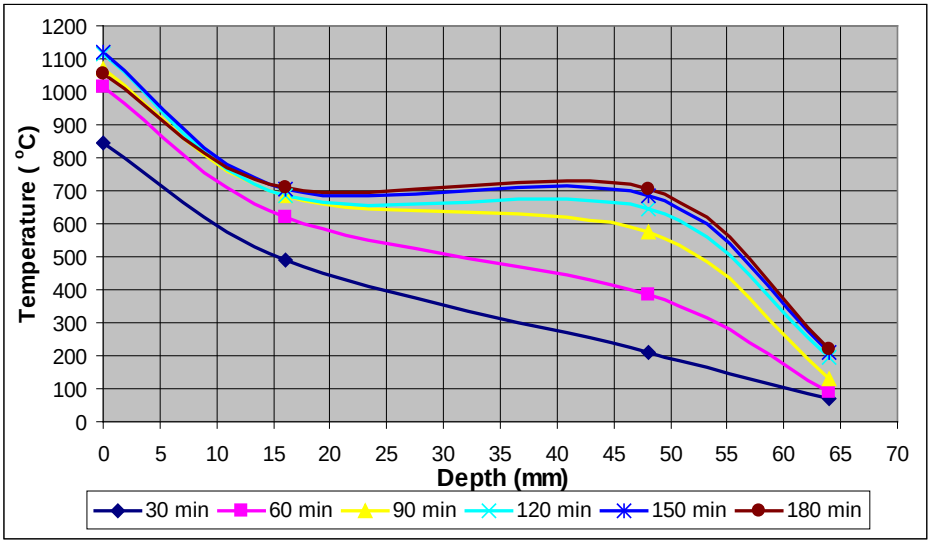

Figure 11: Temperature - Depth Profiles of Test Specimen 6

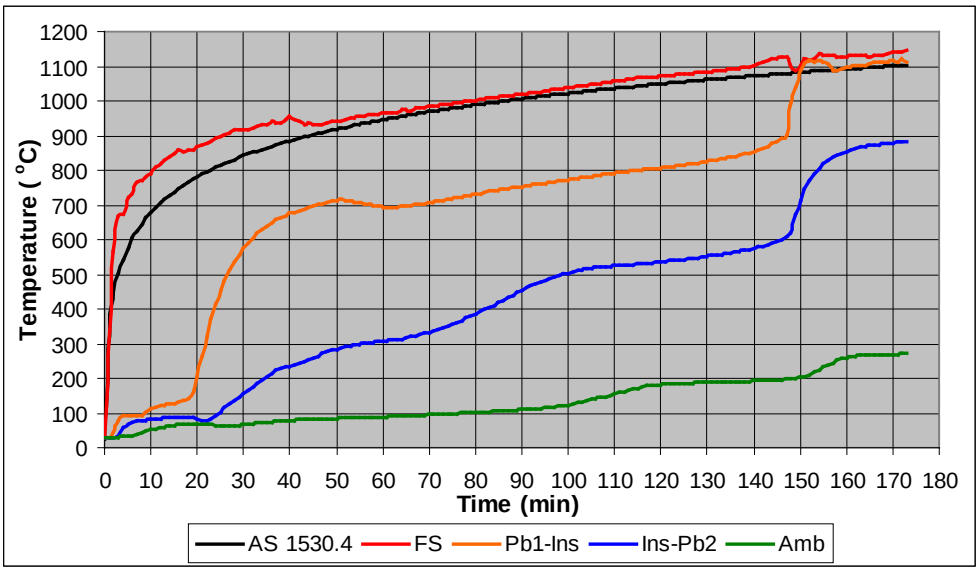

(a) Test Specimen 10

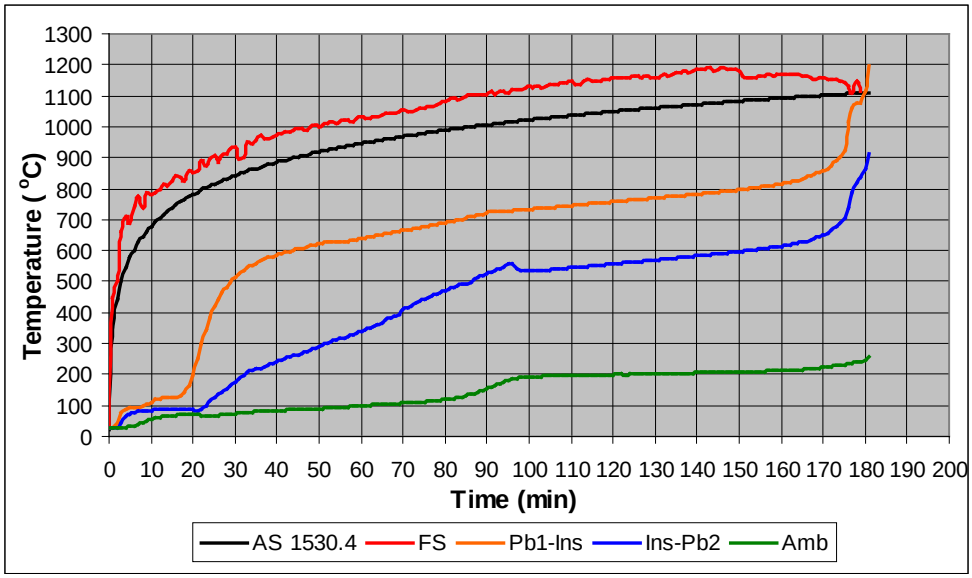

(b) Test Specimen 11

Figure 12: Time - Temperature Profiles of Test Specimens 10 and 11

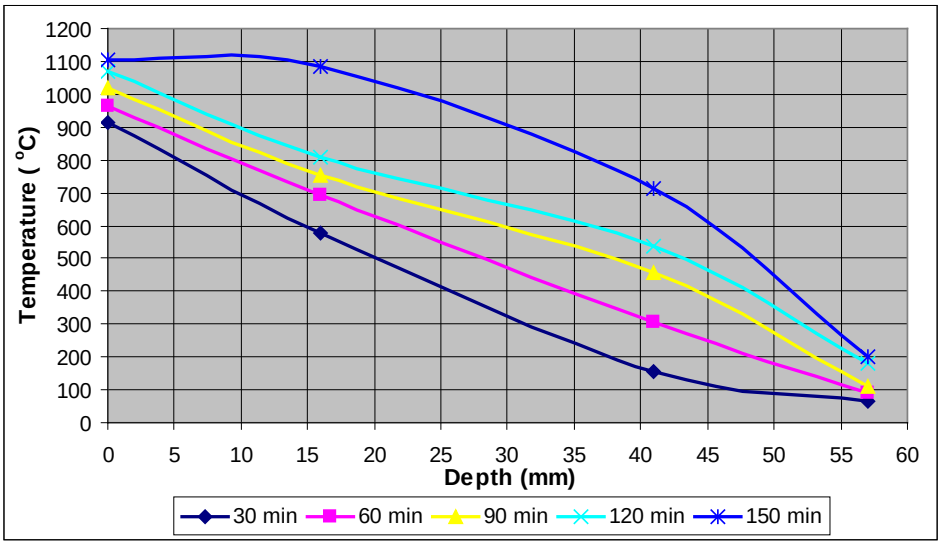

Figure 13: Temperature - Depth Profiles of Test Specimen 10

Rockwool Insulation Intact even after the Fire Test

Figure 14: Fire Testing of Test Specimen 11

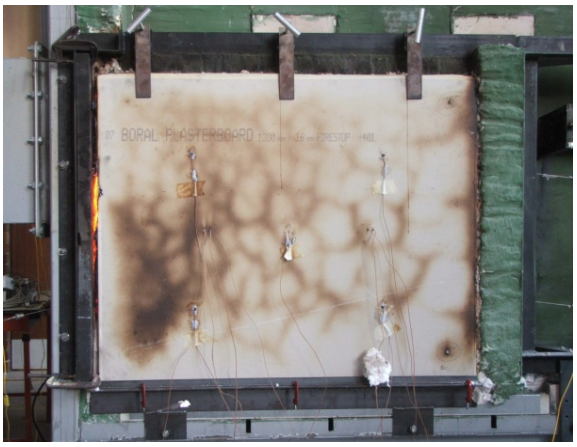

(a) Non-Uniform Discolouration of Paper on the Ambient Side

(b) Burning of Ambient Side Paper

(c) Cellulose Fibre Sample Before and After the Fire Test

Figure 15: Fire Testing of Test Specimen 12

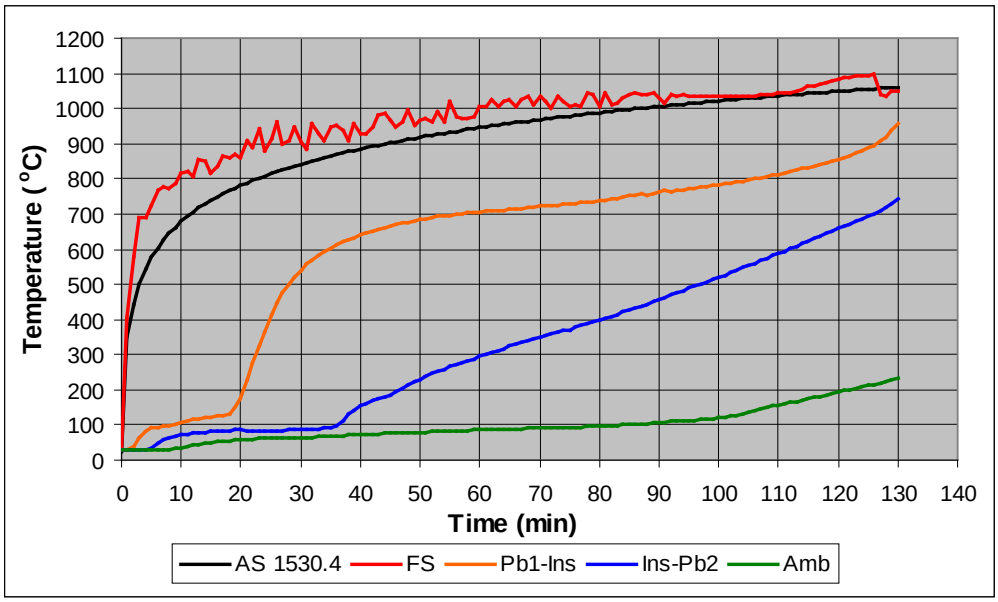

(a) Test Specimen 12

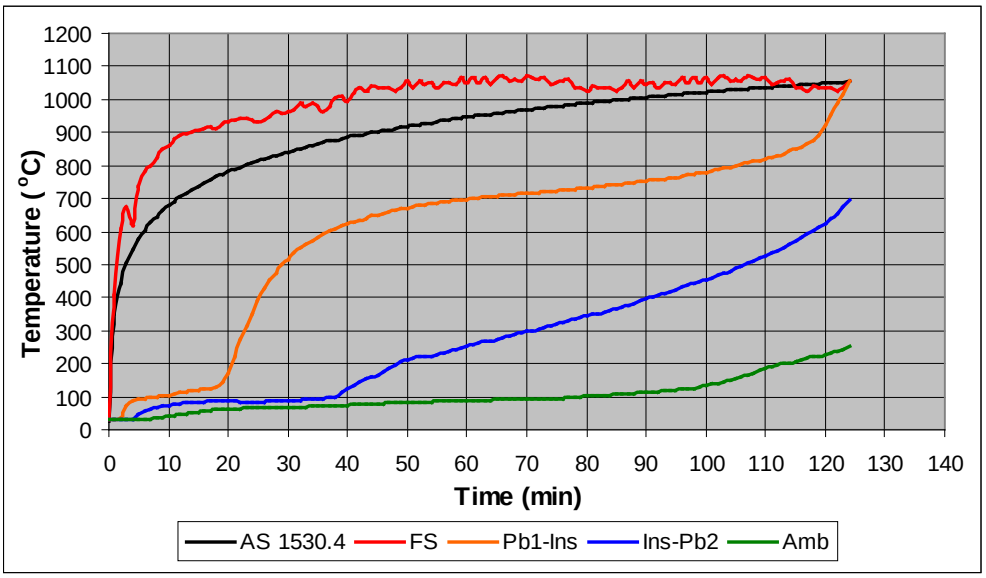

(b) Test Specimen 13

Figure 16: Time - Temperature Profiles of Test Specimens 12 to 14

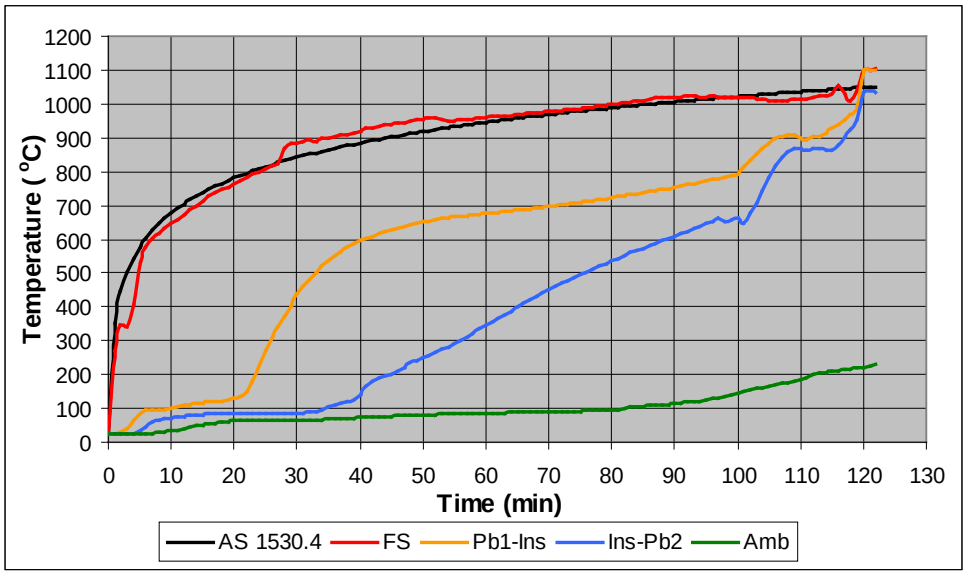

(c) Test Specimen 14

Figure 16: Time - Temperature Profiles of Test Specimens 12 to 14

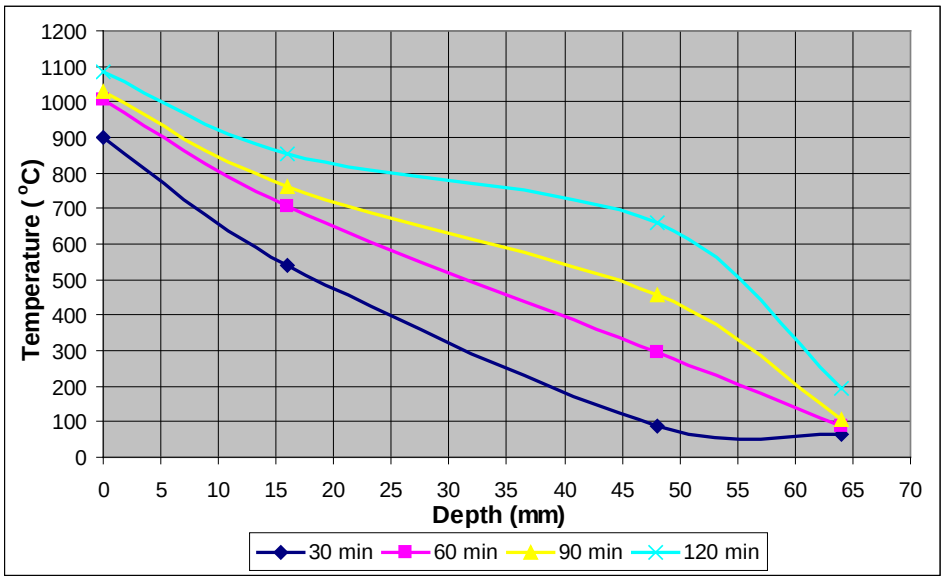

(a) Test Specimen 12

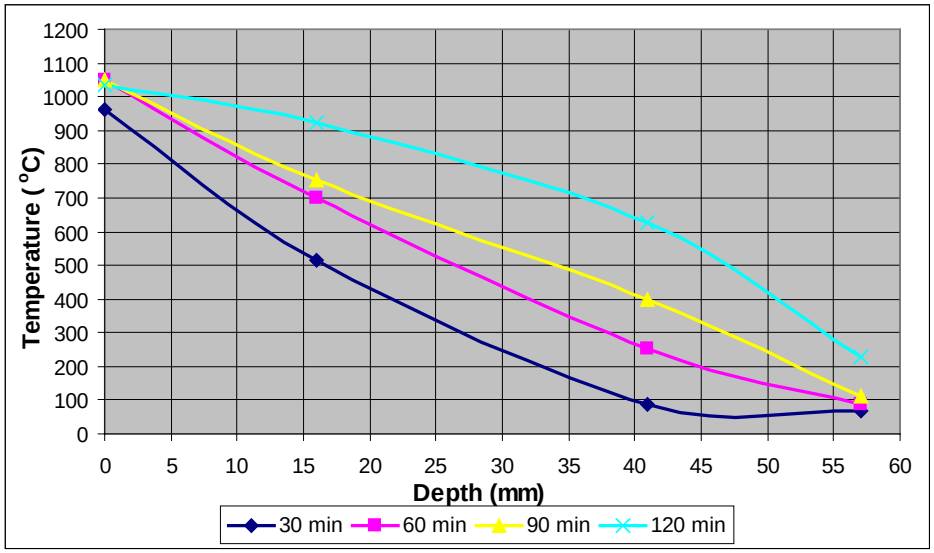

(b) Test Specimen 13

Figure 17: Temperature - Depth Profiles of Test Specimens 12 and 13

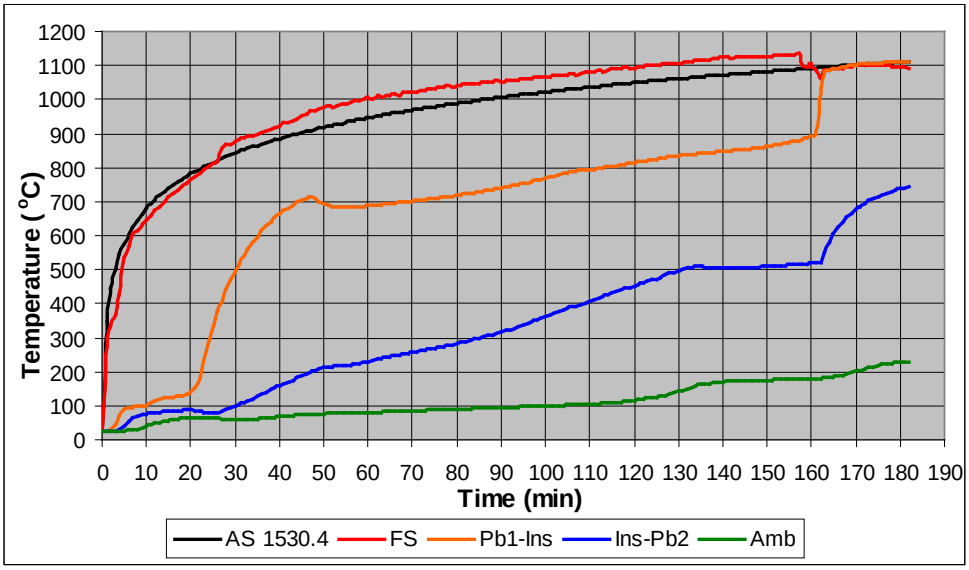

(a) Time - Temperature Profiles

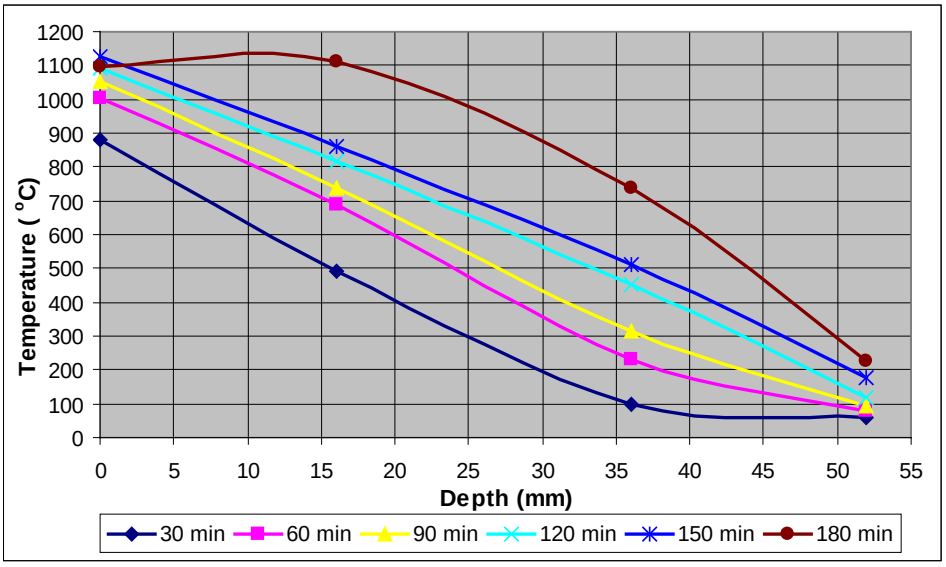

(b) Temperature - Depth Profiles

Figure 18: Temperature Profiles of Test Specimen 15

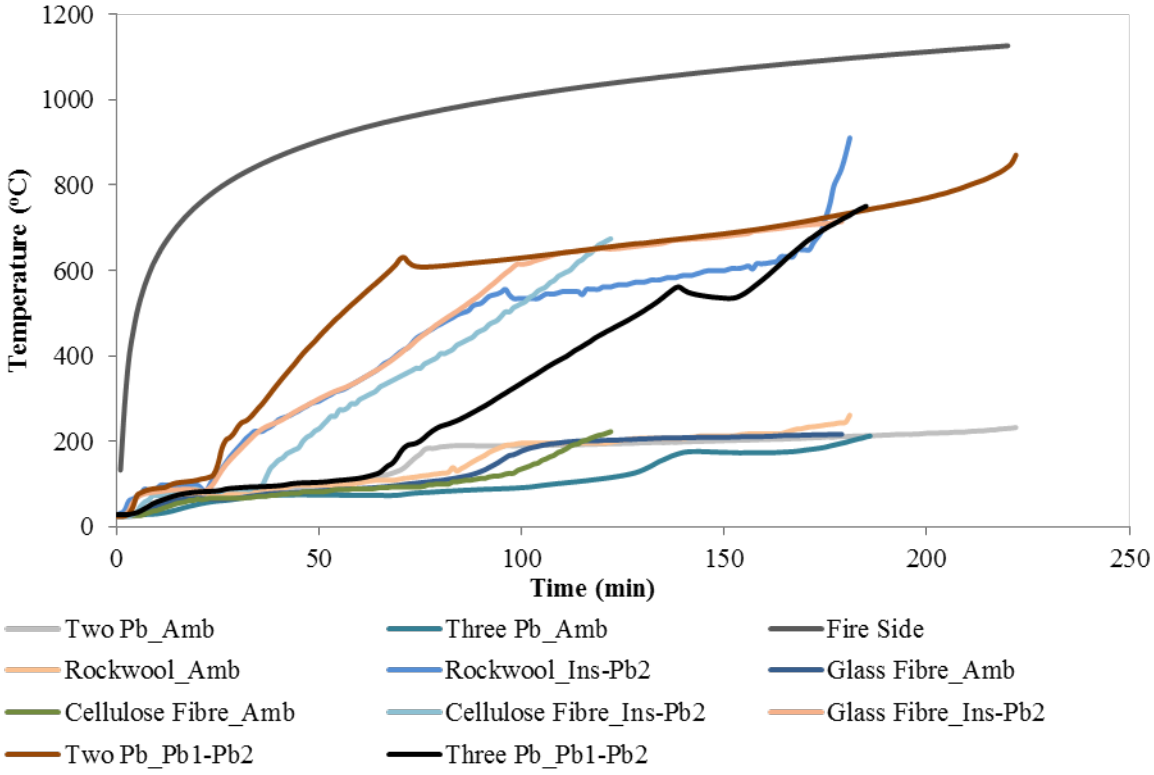

Figure 19: Effect of Using Composite Panels on the Ambient Surface and Interface Time-Temperature Profiles

Table 1: Details of Plasterboard and Composite Panel Test Specimens

No.	Configuration	Specimen Description
1		Pb = 13 mm
2	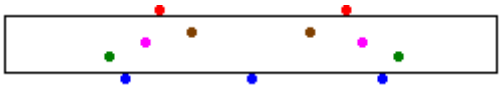	Pb = 16 mm
3	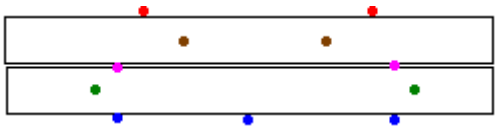	Pb1 = 13 mm (Fire Side) Pb2 = 16 mm (Ambient Side)
4	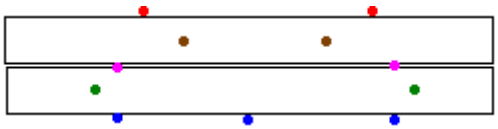	Pb1 = 16 mm (Fire Side) Pb2 = 16 mm (Ambient Side)
5	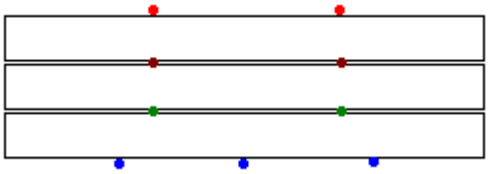	Pb1 = 16 mm (Fire Side) Pb2 = 16 mm (central) Pb3 = 16 mm (Ambient Side)
6, 7, 8, & 9	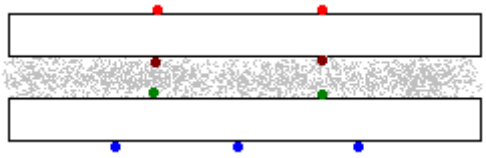	Pb1 = 16 mm (Fire Side) Insulation: Glass Fibre of varying thickness, density and type. Pb2 = 16 mm (Ambient Side)
10 & 11	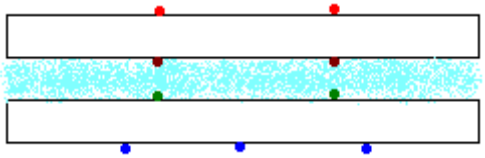	Pb1 = 16 mm (Fire Side) Insulation: Rockwool of varying thickness, density and type. Pb2 = 16 mm (Ambient Side)
12, 13 & 14	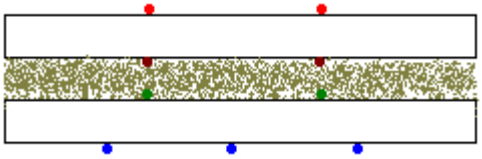	Pb1 = 16 mm (Fire Side) Insulation: Cellulose Fibre of varying thickness, density & type. Pb2 = 16 mm (Ambient Side)
15	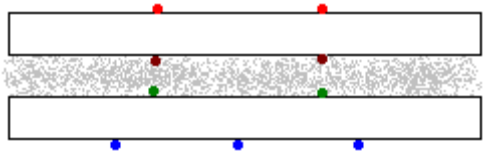	Pb1 = 16 mm (Fire Side) Insulation: Isowool Pb2 = 16 mm (Ambient Side)

Table 2: Time–Temperature Profiles of the Ambient Side of the Insulation (Ins-Pb2 Interface) in Test Specimens 6 to 9 Using Glass Fibre as Insulation Material

Time (min)	Test Specimen 6 t = 32 mm D = 21.7 kg/m^3	Test Specimen 7 t = 32 mm D = 43.4 kg/m^3	Test Specimen 8 t = 25 mm D = 37 kg/m^3	Test Specimen 9 t = 13 mm D = 168 kg/m^3
30	220	190	180	120
40	300	250	240	200
50	350	300	300	250
60	390	320	350	300
70	450	380	410	370
80	520	470	500	430
90	580	540	560	500
100	600	600	660	600
110	620	600	660	700
120	650	600	670	700
130	660	640	660	680
140	680	680	670	670
150	690	690	690	670
160	700	700	700	700
170	710	700	705	720
180	700		720	740

Table 3: Time–Temperature Profiles of the Ambient Side of the Insulation (Ins-Pb2 Interface) in Test Specimens 10 and 11 using Rockwool as Insulation Material

Time (min)	Test Specimen 10 t = 25 mm D = 100 kg/m^3	Test Specimen 11 t = 13 mm D = 114 kg/m^3
30	160	180
40	240	230
50	290	300
60	310	340
70	330	400
80	390	480
90	450	520
100	500	520
110	520	540
120	540	550
130	550	580
140	580	590
150	700	600
160	850	605
170	880	650
180		860

Table 4: Time–Temperature Profiles of the Ambient Side of the Insulation (Ins-Pb2 Interface) in Test Specimens 12 to 14 Using Cellulose Fibre as Insulation Material.

Time (min)	Test Specimen 12 t = 32 mm D = 102 kg/m^3	Test Specimen 13 t = 25 mm D = 108 kg/m^3	Test Specimen 14 t = 20 mm D = 131 kg/m^3
30	90	100	90
40	150	120	140
50	230	205	250
60	300	300	340
70	350	340	450
80	400	340	530
90	460	400	600
100	510	450	650
110	600	520	880
120	670	620	1000